



Groundwater arsenic contamination in Burkina Faso, West Africa: Predicting and verifying regions at risk



Anja Bretzler^{a,d,*}, Franck Lalanne^b, Julien Nikiema^c, Joel Podgorski^a, Numa Pfenninger^a, Michael Berg^a, Mario Schirmer^{a,d}

^a Eawag: Swiss Federal Institute of Aquatic Science and Technology, Dübendorf, Switzerland

^b Institut International d'Ingénierie de l'Eau et de l'Environnement (2iE), Ouagadougou, Burkina Faso

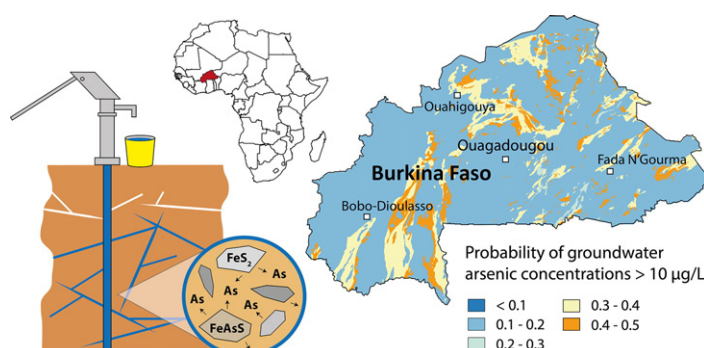
^c Université Ouaga I Pr. Joseph KI-ZERBO, Ouagadougou, Burkina Faso

^d Centre d'Hydrogéologie et de Géothermie (CHYN), Université de Neuchâtel, Switzerland

HIGHLIGHTS

- 14.6% of rural drinking water boreholes in Burkina Faso are affected by arsenic > 10 µg/L.
- Geogenic arsenic is related to sulphide minerals from volcanic rocks and schists.
- Hazard maps pinpoint areas vulnerable to groundwater arsenic contamination.
- ~800,000 people are potentially exposed to drinking water arsenic > 10 µg/L in Burkina.
- Awareness of a transboundary water quality problem affecting the whole region

GRAPHICAL ABSTRACT



ARTICLE INFO

Article history:

Received 29 November 2016

Received in revised form 20 January 2017

Accepted 21 January 2017

Available online 1 February 2017

Editor: Jay Gan

Keywords:

Arsenic contamination

Drinking water

West Africa

Sulphide minerals

Hazard modelling

Health threat

ABSTRACT

Arsenic contamination in groundwater from crystalline basement rocks in West Africa has only been documented in isolated areas and presents a serious health threat in a region already facing multiple challenges related to water quality and scarcity. We present a comprehensive dataset of arsenic concentrations from drinking water wells in rural Burkina Faso ($n = 1498$), of which 14.6% are above 10 µg/L. Included in this dataset are 269 new samples from regions where no published water quality data existed. We used multivariate logistic regression with arsenic measurements as calibration data and maps of geology and mineral deposits as independent predictor variables to create arsenic prediction models at concentration thresholds of 5, 10 and 50 µg/L. These hazard maps delineate areas vulnerable to groundwater arsenic contamination in Burkina Faso. Bedrock composed of schists and volcanic rocks of the Birimian formation, potentially harbouring arsenic-containing sulphide minerals, has the highest probability of yielding groundwater arsenic concentrations > 10 µg/L. Combined with population density estimates, the arsenic prediction models indicate that ~560,000 people are potentially exposed to arsenic-contaminated groundwater in Burkina Faso. The same arsenic-bearing geological formations that are positive predictors for elevated arsenic concentrations in Burkina Faso also exist in neighbouring

* Corresponding author at: Eawag: Swiss Federal Institute of Aquatic Science and Technology, Dübendorf, Switzerland.

E-mail address: anja.bretzler@eawag.ch (A. Bretzler).

countries such as Mali, Ghana and Ivory Coast. This study's results are thus of transboundary relevance and can act as a trigger for targeted water quality surveys and mitigation efforts.

© 2017 Elsevier B.V. All rights reserved.

1. Introduction

Despite the increased construction and development of centralised water distribution systems and piped water supplies in sub-Saharan Africa during the last decades, small-scale groundwater abstraction via hand-dug wells or village hand pumps is often the sole source of drinking water for rural populations (MacDonald et al., 2009; Martin and Van De Giesen, 2005). Especially in the arid and semi-arid regions of the Sahel belt, where surface water resources can dry out completely in the long dry season, rural areas rely on groundwater for their drinking water supply (Edmunds, 2008). In general, groundwater is regarded as having good drinking water quality and to be predominantly free of pathogens, but chemical constituents may present a hazard that is often discovered late or not at all due to insufficient testing and surveying of water quality (MacDonald and Calow, 2009; UNICEF, 2008).

This is the case for arsenic, which can occur naturally in groundwater in concentrations that can lead to serious and chronic health effects after prolonged consumption (Naujokas et al., 2013). Arsenic exposure has not only been linked to the development of a variety of cancers, but also to developmental, neurological, respiratory and cardiovascular effects (Argos et al., 2010; Naujokas et al., 2013; Yuan et al., 2010; Yuan et al., 2007). The World Health Organization (WHO) has imposed a drinking water guideline concentration for arsenic of 10 µg/L, which has also been adopted by Burkina Faso (MAHRH/MS, 2005; WHO, 2011). Large-scale geogenic contamination of groundwater with arsenic in South and Southeast Asia (e.g. Bangladesh, India, Cambodia, Vietnam) has received a lot of attention in the last two decades (e.g. Bhattacharya et al., 1997; Flanagan et al., 2012; Smith et al., 2000; Berg et al., 2007). The phenomenon is still relatively unknown and little studied in West Africa though (Ahoulé et al., 2015), where fractured aquifers composed of weathered crystalline bedrock predominate. This is a totally different system to the young sedimentary aquifers of arsenic-affected regions in Asia, where arsenic is predominantly released by reductive dissolution (Ahmed et al., 2004). Studies in Ghana and Burkina Faso have shown that the oxidation of arsenic-containing sulphide minerals found in rocks of the Birimian formation is the primary process responsible for high arsenic levels found in some groundwater (Asante et al., 2007; Barro-Traoré et al., 2008; Buamah et al., 2008; Sako et al., 2016; Smedley, 1996; Smedley et al., 2007; Somé et al., 2012). However, an understanding of the extent of the problem and a detailed investigation of the sources and geological conditions leading to arsenic contamination is currently lacking.

Since testing wells for arsenic contamination is expensive and time consuming, maps identifying areas that are especially vulnerable to this kind of pollution are largely missing. However, they would be a useful tool for decision makers by helping to focus efforts where they are most needed. Such groundwater vulnerability assessment and mapping is a growing field, with more and more studies focussing on finding methods to assess the vulnerability of aquifers to contaminants such as nitrate or pesticides (Nolan and Hitt, 2006; Nolan et al., 2002; Ouedraogo et al., 2016; Sorichetta et al., 2013).

Specifically concerning arsenic, statistical modelling to predict the spatial occurrence of arsenic and highlight areas where safe drinking water predominates has been performed successfully at different scales, from global to regional, and in a range of different geological terrains (Ahn and Cho, 2013; Amini et al., 2008; Ayotte et al., 2016; Ayotte et al., 2006; Dummer et al., 2015; Rodríguez-Lado et al., 2013; Shamsudduha et al., 2015; Winkel et al., 2008; Winkel et al., 2011; Yang et al., 2012). Fundamental to the development of such models is knowledge of the geochemical processes leading to the occurrence of

high arsenic in groundwater, as well as finding the predictor variables (proxies) to explain these. Since geogenic arsenic is by definition of geological origin, such proxies are usually geological variables, but various environmental parameters, such as temperature or precipitation, that influence geochemical processes in groundwater may also be relevant (Amini et al., 2008).

The concentration of arsenic in groundwater is not only related to the abundance of arsenic found in minerals in the aquifer matrix, it is also a function of solubility, which is governed predominantly by pH and redox conditions (Dixit and Hering, 2003; Hug and Leupin, 2003). In China, for example, Rodríguez-Lado et al. (2013) found elevated groundwater arsenic concentrations in sedimentary basins and river valleys to be strongly associated with Holocene sediments, soil salinity, fine subsoil texture and an elevated Topographic Wetness Index, which functioned as proxies for chemically reducing environments with high arsenic solubility. In the case of arsenic release due to sulphide mineral oxidation in crystalline basement rocks, different proxies must be taken into account, as has been shown by Ayotte et al. (2006), Yang et al. (2012), Ahn and Cho (2013) and Dummer et al. (2015) who modelled a positive correlation between arsenic occurrence and certain mineral-bearing geological formations.

The goal of this study is to investigate the distribution and magnitude of geogenic groundwater arsenic concentrations in Burkina Faso in order to better identify affected areas and populations. We carried out a country-wide arsenic survey and created arsenic prediction models based on three different concentration thresholds (5, 10 and 50 µg/L) taking into account the geochemical processes and conditions responsible for elevated arsenic in groundwater in West Africa. The models were calibrated using a spatially limited arsenic measurement dataset and then validated with measurements from other regions in Burkina Faso to ensure country-wide validity. As is often the case in developing countries, datasets of physical parameters such as geology, hydrogeology, mineral resources and climate were not available to the same extent or resolution as in industrialised nations. For this study, only surface parameters were available. The depth of individual boreholes and lithological logs were not available. Therefore, another goal of this study was to investigate whether a reliable hazard model for arsenic can be produced in light of data scarcity. Due to the large number of countries in the West African region and the difficulty in collecting the necessary data for each individual country, we chose a single “model” country for which to create arsenic prediction models. Burkina Faso was selected because some existing studies already show elevated groundwater arsenic but are limited in their spatial extent (Barro-Traoré et al., 2008; COWI, 2004; Nzihou et al., 2013; Ouedraogo and Amyot, 2013; Sako et al., 2016; Smedley et al., 2007; Somé et al., 2012). The same geological formations that harbour arsenic-containing sulphide minerals in Burkina Faso are also found in neighbouring countries such as Mali, Niger, Ivory Coast, Ghana and Benin (Schlüter, 2008). Therefore, this study is relevant to the greater West African region and should spur increased discussion and mitigation efforts concerning arsenic contamination and its health effects.

2. Hydrological and geological setting and its relevance to elevated arsenic concentrations

Burkina Faso has a hot and dry semi-arid climate, with rainfall restricted to one rainy season per year from June to September. Rainfall is higher in the south-west than in the more arid north and east. Groundwater recharge occurs during the rainy season with smaller total amounts in the north than in the south-west, but can be spatially

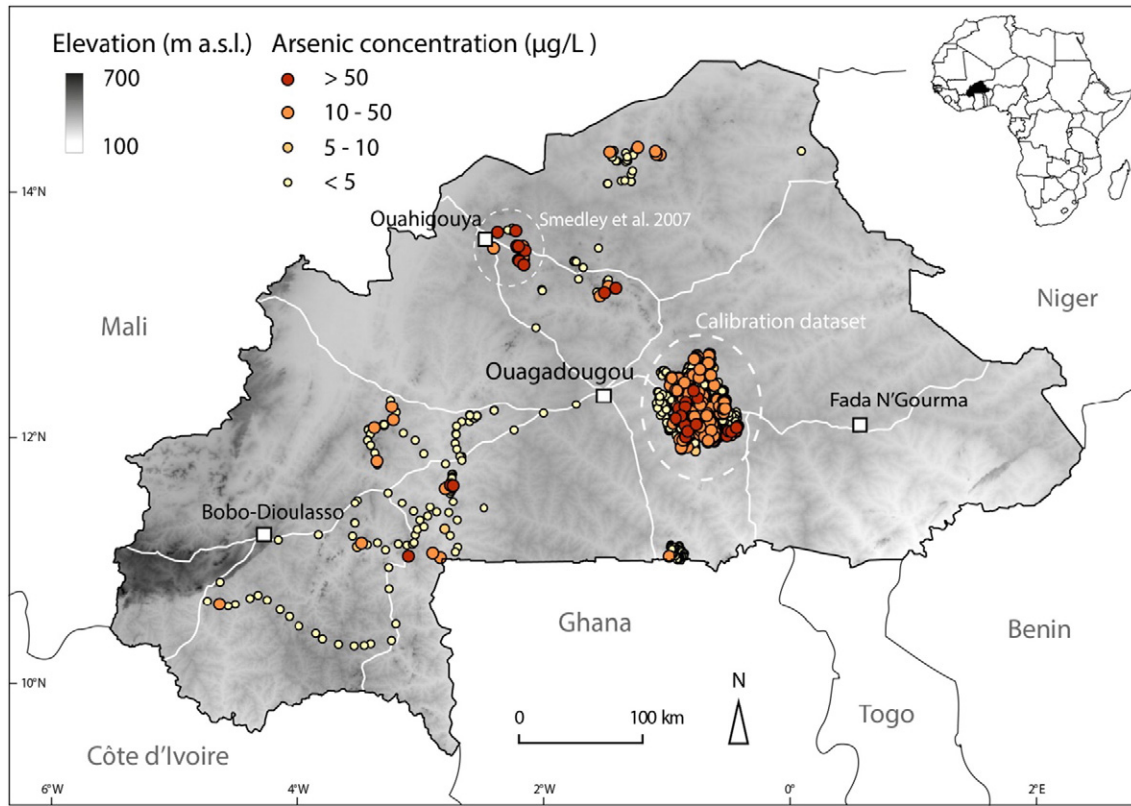


Fig. 1. Overview of the study area, giving the location of groundwater arsenic measurements used in this study (n = 1498). The calibration dataset from the Province of Ganzourgou (source: Unicef/BUMIGEB) is represented by the large cluster of points east of Ouagadougou (n = 1184). The remaining points comprise the validation dataset (n = 314), which includes data from Smedley et al. (2007) (n = 45) and the new measurements presented in this study (n = 269).

highly heterogeneous (Filippi et al., 1990; Martin and Van De Giesen, 2005). Geomorphologically, Burkina Faso is relatively flat, with most of the country lying between 250 and 400 m a.s.l. (Fig. 1). 65% of the land area of Burkina Faso is covered by the Volta basin and is drained

by the Mouhoun, Nazinon and Nakambé rivers (Black, Red and White Volta) (Martin and Van De Giesen, 2005).

Between the in-tact crystalline bedrock at depth and the ground surface, a typical tropical hard-rock weathering profile exists and controls

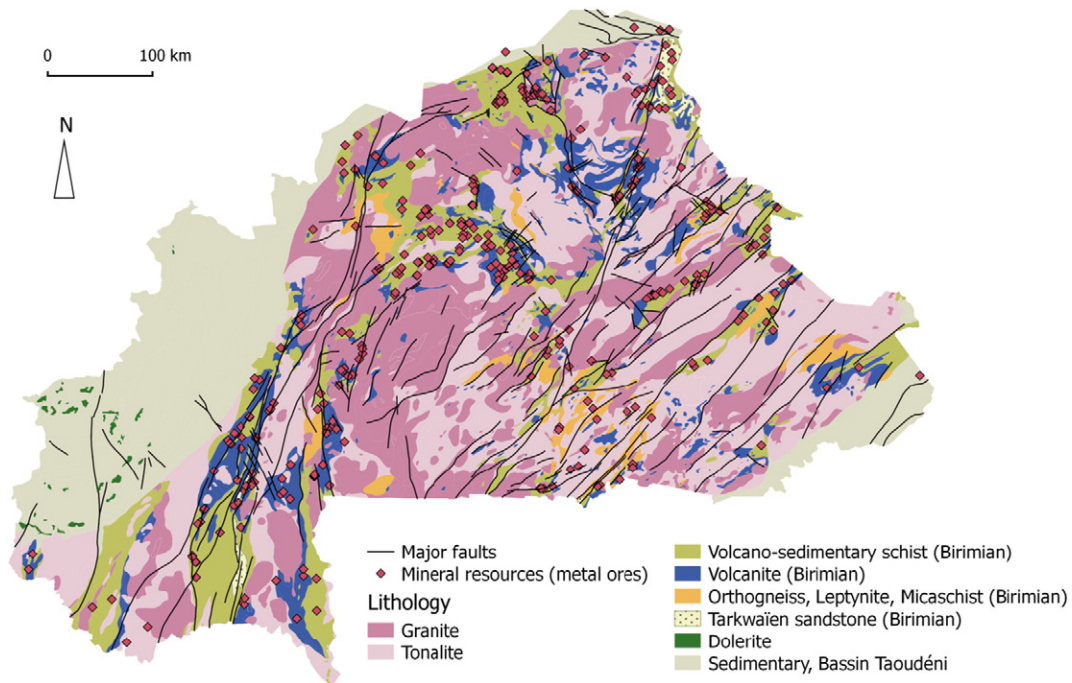


Fig. 2. Simplified geological map of Burkina Faso, showing the main rock types, major faults and the location of mineral deposits (metal ores). Modified from Castaing et al. (2003b).

the local hydrogeological properties, explained in more detail in Courtois et al. (2010) and Nikiema et al. (2013). The top few metres of the ground surface are usually composed of a laterite crust, underlain by a few tens of metres of weathered clayey saprolite, which represents the upper part of the aquifer. This then merges into the so-called fissured layer (densely fissured and fractured weathered bedrock), which can extend to a depth of 80–100 m below ground level and acts as the main aquifer for groundwater storage (Courtois et al., 2010). In rural areas, boreholes for drinking water abstraction with hand pumps are drilled into the fissured layer and have depths ranging from 35 to 90 m. Hand-dug wells tapping shallower aquifers in the weathered saprolite layer may also be used for drinking water purposes.

A large part of Burkina Faso is covered by Paleoproterozoic crystalline basement rocks. These comprise belts of (meta-)volcanic, metasedimentary and plutonic rocks of the Birimian Formation, as well as large intrusive bodies of Eburnean granitoids (granite, tonalite, granodiorite) (Fig. 2). The Birimian volcano-sedimentary belts (also known as Birimian greenstone belts) were formed as part of an island-arc system between 2240 and 2170 Ma. They are composed of varied volcanic and plutonic rocks, including basalt, andesite, rhyolite and gabbro, that occur next to schists, quartzite and chert (Castaing et al., 2003a). The Birimian formation has undergone considerable mineralisation that was synchronous with regional metamorphism and deformation. This led to the formation of high-grade ore deposits, primarily gold and to a lesser extent other metallic ores. Gold deposits principally occur within or adjacent to quartz veins that formed later than the host rock (Béziat et al., 2008). Native gold can occur directly within deformed quartz veins, or as gold particles disseminated in the alteration halos of unfolded quartz veins. Both mineralisation types are directly associated with the occurrence of sulphide minerals such as pyrite (FeS₂) and arsenopyrite (FeAsS) (Béziat et al., 2008; Bourges et al., 1998; Castaing et al., 2003a). Pyrite can incorporate minor and trace elements into its mineral structure and arsenic concentrations in pyrite can occur up to 10 wt% (Abraitis et al., 2004). The oxidation of such sulphide minerals when in contact with oxygen-containing groundwater and subsequent release of arsenic to solution can lead to considerably elevated groundwater arsenic concentrations (Verplanck et al., 2008; Walker et al., 2006; Yang et al., 2015). In general, depending on the redox conditions in the subsurface, arsenic should stay in solution in its reduced form As(III) if reducing conditions are prevalent, but should be tightly adsorbed to iron hydroxides if conditions are oxidising (Dixit and Hering, 2003). Nevertheless, Smedley et al. (2007) measured clearly elevated arsenic concentrations in oxidising groundwater in Burkina Faso and hypothesised that these high concentrations occur in the direct vicinity of mineralised zones where the arsenic loading in groundwater can be very high locally.

3. Methods

3.1. Data collection

3.1.1. Arsenic concentration measurements

A dataset (n = 1498) of georeferenced groundwater arsenic concentration measurements from boreholes in rural areas was used in this study to calibrate and validate the arsenic prediction model (Fig. 1). The dataset includes both new and existing data (Table 1). Included in the 1498 measurements are 269 new groundwater samples taken specifically for this study from 2014 to 2016 in different regions of Burkina Faso (Table 1, Fig. 1). Samples originate from village boreholes equipped with hand pumps (types India, Volanta or Vergnet). We followed standard sampling and laboratory analysis procedures as described in similar studies (Berg et al., 2008; Buschmann et al., 2007). On-site parameters (temperature, pH, electrical conductivity, O₂ concentration and redox potential) were measured in a flow-through cell connected to the pump spout. Water sampling was performed after on-site parameters had stabilised, generally after 5–10 min. All sampled boreholes are

Table 1

Arsenic concentration measurements (n = 1498) used for model calibration and validation.

	Province	No. of samples	% > 10 µg/L As	Source
Calibration data	Ganzourgou	1184	15.5%	Unicef/BUMIGEB
Validation data	Yatenga	45	42% ^a	Smedley et al. (2007)
	Nahouri	52	2%	This study
	Soum	38	13%	This study
	Balé	31	16%	This study
	Various (South-West)	101	9%	This study
	Bam	22	14%	This study
	Boulkiemdé	15	0%	This study
	Various	10	20%	This study

^a Non-random sampling specifically targeting arsenic-affected boreholes.

pumped nearly continuously during the day by local residents for drinking water production, hence water was never stagnant in the pipes during sampling. Samples for major cations and minor and trace element analysis (including arsenic) were collected in acid-washed polypropylene bottles, filtered through 0.45 µm filters and acidified with concentrated HNO₃ suprapure to a pH < 2. An unfiltered, non-acidified aliquot was collected for analysis of anions, DOC and TIC. Samples were stored below 4 °C whenever possible. Analysis was performed in the laboratories of Eawag, Switzerland, using ICP-MS (Agilent 7500cx) for cations and trace elements, ion chromatography for anions (ICS-2001 Dionex) and a carbon analyser (TOC Shimadzu) for TIC and DOC.

Also included in the total dataset of 1498 samples are 1184 arsenic measurements obtained through a study commissioned by Unicef Burkina Faso and carried out by the “Bureau des Mines et de la Géologie du Burkina” (BUMIGEB) in 2010 to measure arsenic concentrations in drinking water boreholes in the Province of Ganzourgou, 50 km east of Ouagadougou. Samples were measured in the laboratories of BUMIGEB using Atomic Absorption Spectroscopy (AAS). Depths of individual boreholes are not known, however a separate database of 434 boreholes from Ganzourgou contains depths ranging from 35 to 90 m, with a mean of 51 m. In addition to the Ganzourgou data, 45 arsenic measurements from the Ouahigouya region (Yatenga Province) in northern Burkina Faso were provided by Smedley et al. (2007).

3.1.2. Model variables

3.1.2.1. Independent predictor variables. Georeferenced map data with a country-wide coverage were considered as predictor variables for the arsenic prediction model. As groundwater arsenic in Burkina Faso is thought to originate from sulphide minerals in mineralised zones, focus was set on assembling predictor variables that could indicate such mineralisation, such as lithological variables and distances to mineral deposits, faults and granitic intrusions (Table 2). The Geological and Mineral Deposit Map of Burkina Faso at a scale of 1:1,000,000 (Castaing et al., 2003b) was used to extract major lithologies, faults and the location of mineral deposits of metal ores (e.g. gold, zinc, chromium, manganese) (Fig. 2). In addition to the location of mineralised zones, groundwater flow and residence time may also play a role in arsenic concentrations. Due to the heterogeneity of fractured bedrock aquifers, mapping such parameters on a regional or country-wide scale is problematic (Dewandel et al., 2012). As possible proxies for hydrological processes related to groundwater flow and residence time we chose the “drainage direction” and “flow accumulation” datasets of the HydroSHEDS database (Lehner et al., 2008). These data are derived from the digital elevation model (DEM) of the Shuttle Radar Topography Mission (SRTM).

The predictor data layers were converted to raster format (if originally in vector format such as polygon, line or point) with a resolution

Table 2
Predictor variables used in the arsenic prediction model.

Predictor variables	Type	Format	Source
Volcano-sedimentary schist (Birimian)	Categorical	Polygon	BUMIGEB/BRGM (Castaing et al., 2003b)
Volcanite: basalt, andesite, rhyolite (Birimian)	Categorical	Polygon	
Orthogneiss (Birimian)	Categorical	Polygon	
Granite	Categorical	Polygon	
Tonalite	Categorical	Polygon	
Distance to faults	Continuous	Raster	
Distance to mineral deposits (metal ores)	Continuous	Raster	
Distance to granitoid rocks	Continuous	Raster	
Drainage direction	Continuous (30 arc sec)	Raster	HydroSHEDS/WWF, (Lehner et al., 2008)
Flow accumulation	Continuous (30 arc sec)	Raster	

of 30 arc sec (1 km on the equator) using standard tools available in the open source QGIS and GRASS software packages (GRASS Development Team, 2015; QGIS Development Team, 2015). The distances to faults, mineral deposits, and granitoid rocks were calculated within a buffer zone of a maximum of 10 km away from the feature.

3.1.2.2. Dependent variable (arsenic concentration measurements). In order to be compatible with the predictor variables, the calibration dataset of arsenic concentration measurements was converted from point to raster format and concentrations aggregated to one value per 1 km² pixel by using the maximum arsenic concentration if more than one measurement fell into the pixel. We chose the more conservative maximum value instead of averaging concentrations in order to ensure that high-arsenic boreholes remain in our analyses and are not “diluted” by surrounding low concentrations. As such, the original calibration dataset of 1184 individual arsenic measurements was reduced to 877 measurements, with 39% above 5 µg/L, 19% above 10 µg/L and 2% above 50 µg/L. The aggregated concentration values were binary-coded according to the chosen threshold (above threshold = 1, below threshold = 0) and used as the dependent variable in the logistic regression model. We chose the threshold values of 5, 10 and 50 µg/L to represent the full concentration range of the dataset. Furthermore, 10 µg/L is the WHO and national drinking water guideline value and therefore of greatest relevance for drinking water. Discussions also exist in Burkina Faso of raising the guideline value to 50 µg/L, a value that is used in some other arsenic-affected countries, such as Bangladesh. The calibration dataset from Ganzourgou Province has a limited spatial extent (4000 km²) but very dense borehole coverage within this area. All predictor variables are present in this zone and any potential spatial bias is therefore limited. On the other hand, the validation dataset (composed of the 269 new samples described in this study, plus 45 samples from Smedley et al. (2007)), is spatially well distributed and includes locations from the north, south and west of Burkina Faso (Fig. 1).

3.2. Geospatial hazard modelling

Logistic regression was used to model the probability of arsenic occurring over three concentration threshold values. This method is extensively used in a variety of fields to determine the relationship between a binary dependent outcome variable and a number of independent predictor variables (Hosmer et al., 2013). Specifically, logistic regression models the log(odds), which is defined as the probability P that an event occurs relative to the probability that it fails to occur $(1 - P)$, (e.g. arsenic being above/below the threshold concentration), as the linear combination of a set of independent predictor variables

$(x_1..x_k)$ with model coefficients $\beta_1..,\beta_k$ (Hosmer et al., 2013).

$$\log(\text{odds}) = \log\left(\frac{P}{1-P}\right) = \beta_0 + \beta_1x_1 + \dots + \beta_kx_k$$

Removing the logarithm then gives the probability:

$$P = \frac{e^{(\beta_0 + \beta_1x_1 + \dots + \beta_kx_k)}}{1 + e^{(\beta_0 + \beta_1x_1 + \dots + \beta_kx_k)}}$$

The exponential of the model coefficients $\exp(\beta)$ being > 1 indicates an increasing effect of the predictor variable on the dependent variable, while a value < 1 denotes a decreasing effect.

Logistic regression modelling was carried out within the R statistical environment (R Core Team, 2015). We have followed similar procedures as described in detail in Rodríguez-Lado et al. (2013). Univariate logistic regressions for the three chosen thresholds of 5, 10 and 50 µg/L were performed separately on each predictor variable using the whole calibration dataset as the dependent variable. The drainage direction and flow accumulation datasets were discarded from further analyses as they did not prove to be significant predictors for elevated arsenic at the 95%-confidence level in the univariate models (p -values > 0.05) (Table 3). The orthogneiss, tonalite and “distance to faults” predictors were also not significant (Table 3), but were nevertheless kept for further analyses. Orthogneiss belongs to the partly mineralised Birimian formation and could potentially be linked to arsenic contamination, tonalite is a widespread rock type in Burkina Faso with a large spatial coverage (Fig. 2) and fault zones as areas of increased fracturing and/or deformation are also hypothesised to be potential proxies for mineralised zones.

The remaining eight predictor variables were used for multivariate logistic regression. Instead of single-algorithm models, which are vulnerable to the number and location of the calibration data, we chose to create an ensemble model from numerous base models (ensemble members) for more robust results (Rodríguez-Lado et al., 2013). The calibration dataset was randomly split into training (75%) and testing (25%) portions for multivariate logistic regression with stepwise selection (both directions), whereby predictor variables are automatically retained or removed according to the Akaike Information Criterion (AIC) (Akaike, 1974). This procedure was repeated 100 times, creating 100 models each calculated with a different subset of training data. These models were then used to calculate probabilities for the testing data subsets, whereby the Hosmer-Lemeshow goodness-of-fit test at the 95%-confidence level was applied to assess the accuracy of the model, i.e. whether the model is consistent with the testing data that were not used to calibrate it (Hosmer et al., 2013). Models with a significant Hosmer-Lemeshow test ($p < 0.05$) indicate that there is no relationship between predicted and observed data. Models with a high p -values ($p > 0.05$) in this test were therefore retained. Of the remaining ensemble members, a weighted mean of the model coefficients ($\beta_1..,\beta_k$)

Table 3

Results of univariate logistic regression models for three concentration thresholds. Significant values at the 95%-confidence level ($p < 0.05$) are highlighted in bold font.

Predictor variables	p-Values		
	5 µg/L	10 µg/L	50 µg/L
Volcano-sedimentary schist (Birimian)	<0.001	<0.001	<0.001
Volcanite: basalt, andesite, rhyolite (Birimian)	0.01	<0.001	0.99
Orthogneiss (Birimian)	0.22	0.15	0.99
Granite	0.002	<0.001	0.01
Tonalite	0.40	0.06	0.44
Distance to faults	0.67	0.42	0.19
Distance to mineral deposits (metal ores)	<0.001	0.87	0.02
Distance to granitoid rocks	<0.001	<0.001	<0.001
Drainage direction	0.14	0.63	0.31
Flow accumulation	0.59	0.81	0.93

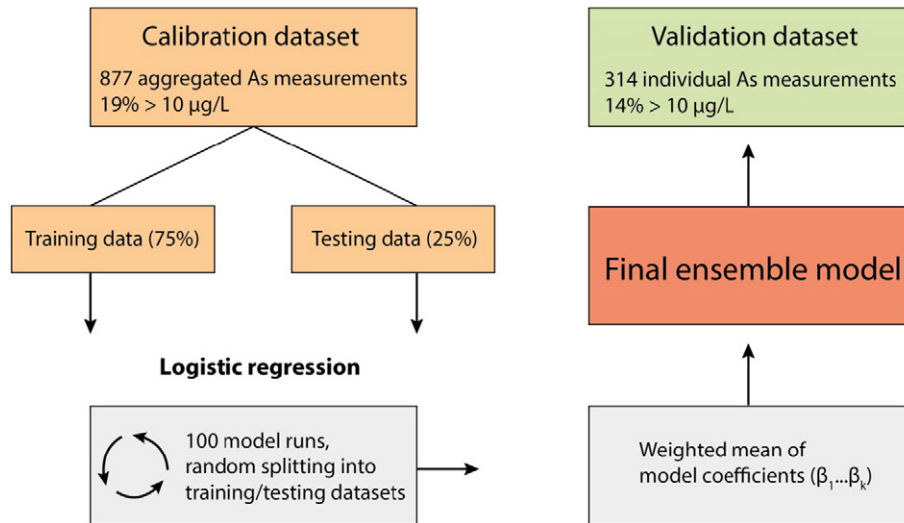


Fig. 3. Overview of the logistic regression modelling procedure.

was calculated to generate a final ensemble model for each of the three threshold concentrations. Weighting was applied according to the frequency that a predictor variable was retained by stepwise selection in

the ensemble members. In this way, predictor variables that occurred frequently in many ensemble members received a higher weighting and greater relative importance in the final ensemble model than

Table 4
Summary results of field and laboratory analyses performed on new groundwater samples.

Parameter	Unit	Minimum	Maximum	Mean	Median	St.Dev	n	WHO guideline	% > guideline
pH	–	4.85	8.18	6.75	6.86	0.45	221	–	–
EC	µS/cm	26.0	2311	369	339	219	220	–	–
O ₂	mg/L	0.40	6.26	2.22	2.01	1.13	134	–	–
Temp	°C	26.7	33.0	30.9	31.0	0.98	221	–	–
Eh	mV	69	305	250	281	64	21	–	–
DOC	mg/L	0.25	3.1	0.42	0.25	0.48	269	–	–
TIC	mgC/L	1.5	112	42	39	22	269	–	–
HCO ₃	mg/L	7.5	560	212	197	110	269	–	–
F	mg/L	<0.1	2.55	0.28	0.19	0.36	269	1.5	2.6
Cl	mg/L	<0.1	129	4.11	1.23	10.8	269	–	–
Br	mg/L	<0.1	0.63	0.07	0.05	0.06	269	–	–
NO ₃	mg/L	<0.1	1060	17.8	4.6	69.7	269	50	5.6
SO ₄	mg/L	<0.1	1250	9.90	0.83	80.9	244	–	–
PO ₄	mg/L	<0.1	14.8	0.18	0.05	0.99	244	–	–
Li	µg/L	<0.1	94.2	15.9	11.9	15.0	269	–	–
B	µg/L	<5	332	13.0	5.6	31.5	269	2400	–
Na	mg/L	0.7	172	21.6	18.2	16.4	269	–	–
Mg	mg/L	0.2	110	14.9	13	11.8	269	–	–
Al	µg/L	<0.1	1952	13.1	1.5	119	269	900 (HB)	0.3
Si	mg/L	5.2	53.3	26.7	25.5	10.4	269	–	–
K	mg/L	0.16	45.0	2.41	1.51	3.75	269	–	–
Ca	mg/L	0.6	318	30.8	27.3	30.2	269	–	–
V	µg/L	<0.02	67.5	9.63	6.78	10.6	269	–	–
Cr	µg/L	<0.02	13.6	0.54	0.15	1.25	269	50	0
Mn	µg/L	<0.02	1101	26.8	4.77	83.9	269	400 (HB)	–
Fe	µg/L	<0.3	6043	155	7.35	548	269	–	–
Co	µg/L	<0.02	4.71	0.19	0.04	0.50	269	–	–
Ni	µg/L	<0.02	9.51	0.74	0.38	0.99	269	70	0
Cu	µg/L	<0.1	31.7	1.77	0.66	3.37	269	2000	0
Zn	µg/L	<0.1	3187	62.0	7.85	247	269	–	–
As	µg/L	<0.02	421	7.56	0.4	38.8	269	10	9.6
Se	µg/L	<0.02	4.32	0.32	0.09	0.64	269	40	0
Sr	µg/L	8	3048	259	182	312	269	–	–
Mo	µg/L	<0.02	144	3.53	0.86	14.3	269	70 (HB)	1.1
Cd	µg/L	<0.01	3.94	0.04	0.005	0.25	269	3	0.3
Sb	µg/L	<0.01	16.7	0.20	0.05	1.02	269	20	0
Ba	µg/L	<0.1	539	53.6	15.3	81.4	269	700	0
La	µg/L	<0.01	0.59	0.04	0.01	0.08	269	–	–
Ce	µg/L	<0.01	1.06	0.06	0.014	0.15	269	–	–
W	µg/L	<0.02	9.97	0.31	0.075	0.84	269	–	–
Tl	µg/L	<0.02	0.37	0.02	0.01	0.03	269	–	–
Pb	µg/L	<0.02	8.28	0.25	0.06	0.72	269	10	0
Th	µg/L	<0.01	<0.01	<0.01	<0.01	0.00	269	–	–
U	µg/L	<0.02	8.96	0.21	0.01	0.90	269	30	0

HB: health-based value, no formal guideline value established.

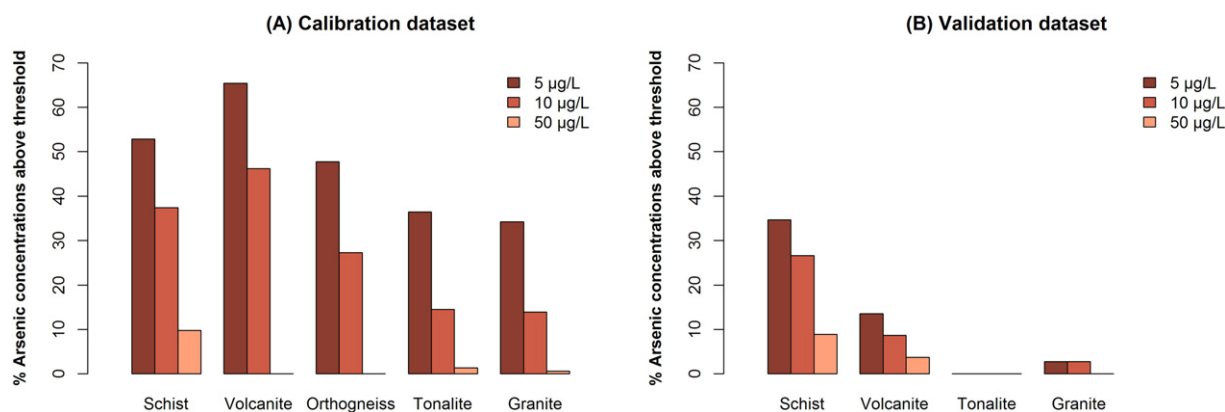


Fig. 4. Bar graphs showing the distribution of arsenic concentrations above the chosen threshold value in relation to the lithology of the aquifer. A) displays the calibration dataset (aggregated to one arsenic value per 1 km² pixel as was used for modelling, n = 877), B) the validation dataset (n = 314). The rock type “Orthogneiss” does not occur in areas where water was sampled for the validation dataset and is therefore not represented on the graph on the right.

variables that were retained in relatively few ensemble members. Variables that were present in <5 out of a maximum of 100 ensemble members were not considered for the final model. See Fig. 3 for a summary of the above-mentioned procedure. A Receiver Operating Characteristics (ROC) curve was computed on the final ensemble model using the whole calibration dataset to assess how well the model discriminates between low and high risk observations (Fawcett, 2006). For this, the rate of true positives (sensitivity) was plotted against the rate of true negatives (specificity) and the area under the curve (AUC) computed. An AUC value of 0.5 denotes a model that is no better than a random model, and a value of 1 would be a perfect prediction.

3.3. Hazard map generation

The final model coefficients were used to generate hazard maps showing the modelled probability of groundwater arsenic concentrations exceeding the threshold concentrations of 5, 10 and 50 µg/L. The cut-off value to distinguish between low- and high-risk areas was chosen where the sensitivity and specificity of the model were equal (Rodríguez-Lado et al., 2013; Winkel et al., 2008). To calculate how many people are potentially affected by elevated arsenic in their drinking water, we combined the hazard map with population density estimates obtained from the Center for International Earth Science Information Network - CIESIN - Columbia University (2016).

4. Results and discussion

4.1. Arsenic concentration data

The full chemical analysis performed on the 269 new groundwater samples presented in this study will only be discussed briefly here to give a broad overview of water chemistry. Results are summarised in Table 4 and show that groundwater is generally near-neutral in pH, contains dissolved oxygen and is largely of good chemical quality for drinking.

Arsenic is by far the contaminant of greatest concern, with 9.6% of samples above the WHO and national guideline value of 10 µg/L. Arsenic speciation measurements were carried out on few samples (n = 31) from the Province of Balé, about 180 km south-west of Ouagadougou and show that arsenic is predominantly present as As(V), confirming the findings of Smedley et al. (2007). No other trace elements show significantly high concentrations and dissolved iron concentrations are typically very low. Nitrate concentrations are high in some boreholes, with 5.6% of samples above the WHO guideline value of 50 mg/L (Table 4). Drinking water boreholes are generally located in the immediate vicinity of human dwellings and are also used for watering livestock, therefore human and animal waste is a likely source of nitrate to groundwater (Huneau et al., 2011; Nikiema et al., 2010). Geogenic fluoride contamination is restricted to the southern province of Nahouri close to the village of Tiébélé, where the fluoride concentrations of only a few samples were slightly above the WHO guideline value of 1.5 mg/L.

Table 5
Weight-averaged coefficients (β), standard deviation and frequency per 100 model runs of predictor variables that were retained in the final ensemble models. The averaged p-value of the Hosmer-Lemeshow (HL) goodness-of-fit test for the significant ensemble members is given in the last column (p-values ≤ 0.05 were discarded).

Predictor variables	Coefficient β	Exp(β)	St. dev.	Freq. in analyses	p-Value HL test
5 µg/L threshold					
Volcano-sedimentary schist (Birimian)	0.7	2.01	0.12	89	0.87
Volcanite (Birimian)	1.19	3.29	0.24	90	
Orthogneiss (Birimian)	0.33	1.39	0.35	46	
Distance to granitic intrusions	0.04	1.03	0.76	6	
10 µg/L threshold					
Volcano-sedimentary schist (Birimian)	1.3	3.67	0.11	98	0.91
Volcanite (Birimian)	1.68	5.37	0.26	98	
Orthogneiss (Birimian)	0.74	2.1	0.2	83	
50 µg/L threshold					
Volcano-sedimentary schist (Birimian)	2.82	16.77	0.54	27	0.93
Tonalite, granodiorite	0.48	1.61	1.37	8	

(Table 4). This region is directly adjacent to Bongo district of northern Ghana, where geogenic fluoride contamination originating from alkaline granitic rocks has been extensively documented (Alfredo et al., 2014; Apambire et al., 1997; Salifu et al., 2012).

The complete arsenic concentration dataset of 1498 measurements demonstrates that elevated levels of arsenic in groundwater are found in numerous provinces (Fig. 1, Table 1) and are not restricted to northern Burkina Faso where most previous studies were carried out (Barro-Traoré et al., 2008; Smedley et al., 2007; Somé et al., 2012). Of all 1498 collected measurements, 14.6% contained arsenic concentrations above the national and WHO guideline value of 10 µg/L and 2.3% above 50 µg/L. 84% of elevated arsenic concentrations (those above 10 µg/L) fall into the range of 10–50 µg/L, and very high concentrations

(above 50 µg/L), which are especially relevant to people's health, are much less frequent.

4.2. Arsenic and lithology

Fig. 4 shows the percentage of samples above the given arsenic thresholds according to the host rock type. Although arsenic concentrations above 5 µg/L are found in all rock types with only a slight preference for Birimian lithologies, those above 10 and 50 µg/L are increasingly more likely to be only found in volcano-sedimentary schists and volcanic rocks (basalt, andesite, rhyolite) of the Birimian formation and are much less common in groundwater from granitic rocks (granite, tonalite, granodiorite). This supports findings from previous

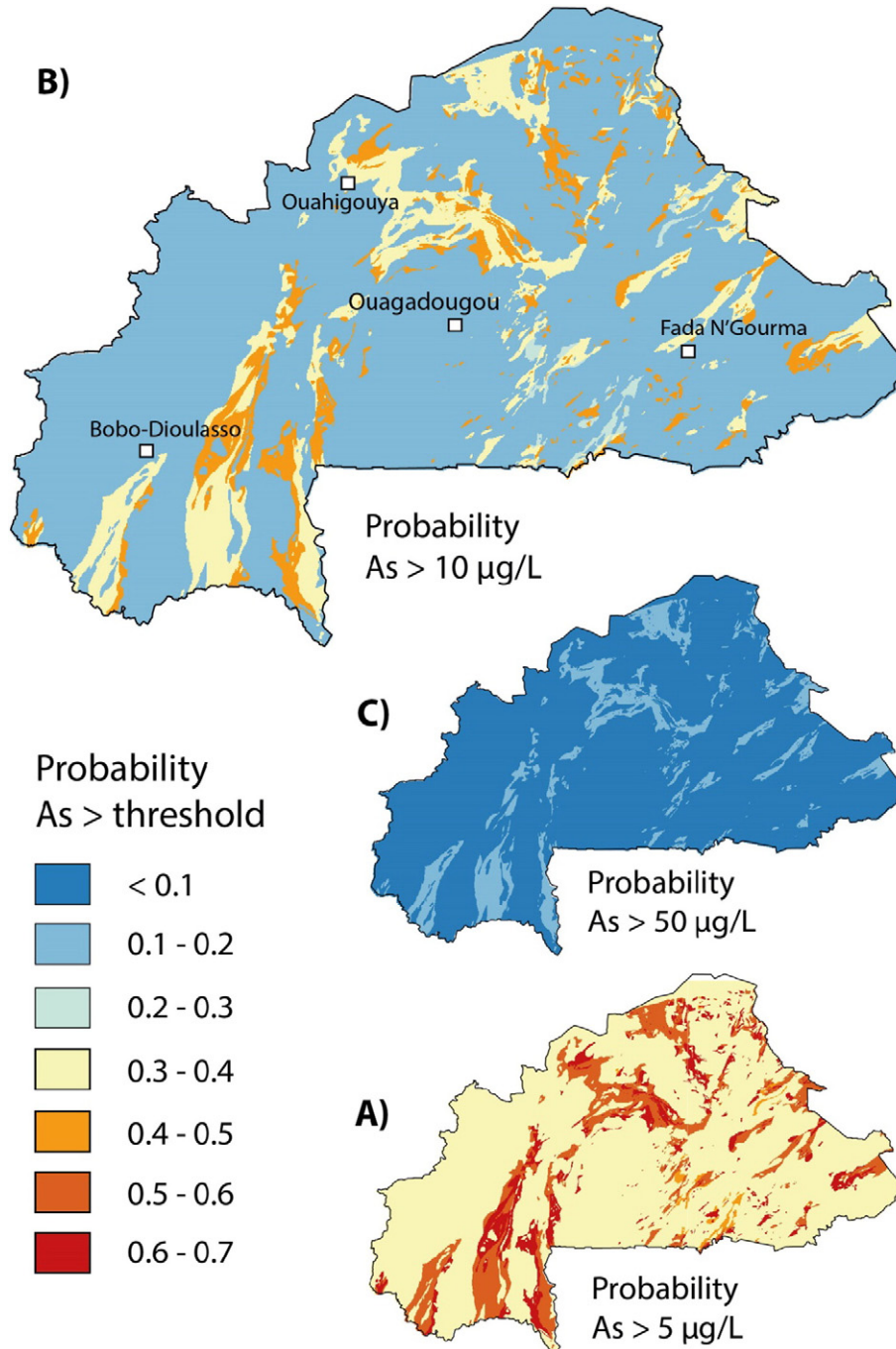


Fig. 5. Modelled probability of groundwater arsenic concentrations exceeding the threshold values of A) 5 µg/L, B) 10 µg/L and C) 50 µg/L.

studies (e.g. Smedley et al. (2007)) that arsenic is linked to the occurrence of sulphide minerals in volcano-sedimentary rocks of the Birimian formation. Geogenic arsenic in groundwater is much less common in granitic areas, which have not undergone widespread alteration or hydrothermalisation processes leading to the formation of mineral deposits.

Arsenopyrite and pyrite occurrence in the Birimian greenstone belts has been documented in numerous studies, e.g. Milési et al. (1992), Béziat et al. (2008). Unfortunately, data on arsenic concentrations in pyrite minerals in Burkina Faso were not available. A database of geochemical analyses of 482 rock samples taken throughout Burkina Faso in both granitic and volcanic/metamorphic terranes (Castaing et al., 2003a) showed few samples ($n = 27$) that had arsenic concentrations greater than the upper crustal abundance of 5.7 mg/kg given in Hu and Gao (2008). All of these high-As samples were located within the Birimian greenstone belts and were volcanic, meta-volcanic or meta-sedimentary rocks, with the highest arsenic concentration of 55 mg/kg being measured in a meta-basalt sample. Arsenic in groundwater can be assumed to originate from sulphide minerals in such rocks, however identifying the sources of high concentrations in specific boreholes would require very local, in-depth geochemical studies with rock samples ideally being taken during borehole drilling.

Groundwater arsenic concentrations are subject to a great degree of spatial variability, with arsenic-affected wells often in direct proximity to “safe” wells. This effect is observed in nearly all arsenic-affected areas worldwide, regardless of the geological setting and arsenic mobilisation mechanism and indicates that arsenic concentration in groundwater is influenced by very local, small-scale conditions (Fendorf et al., 2010; Van Geen et al., 2003). In Burkina Faso, the occurrence of potentially arsenic-containing sulphide minerals (e.g. pyrite, arsenopyrite) is linked to gold-bearing quartz veins that are heterogeneously distributed within the volcano-sedimentary schists and volcanic rocks of the Birimian belts. The occurrence of sulphide minerals can therefore vary over a scale of metres, depending on the size of mineralised veins. Smedley et al. (2007) hypothesised that As(V) may reach high dissolved concentrations in direct proximity to these mineralised zones, where it may be in equilibrium with secondary Fe-oxides having high sorbed As(V) loads. In addition, groundwater may flow in fractures that are totally isolated from each other. It is plausible that anoxic/suboxic zones may develop in such fractures, locally favouring the desorption of As(III) bound to Fe-oxides as has been suggested by Yang et al. (2015). Whether a borehole intercepts a groundwater flow path very close to a mineralised zone is likely the main factor affecting whether or not elevated arsenic is present in the well.

4.3. Predicting arsenic-affected areas

Logistic regression was performed on the calibration dataset for the three chosen thresholds using eight explanatory variables as predictors for elevated groundwater arsenic occurrence. For all three thresholds, only some of the lithological variables were significantly related to the presence of elevated arsenic as shown by the mean model coefficients (Table 5), whereas the distance variables (faults, mineral deposits, granitic intrusions) did not have a significant influence on the final ensemble model. Volcano-sedimentary schists of the Birimian formation increase the odds of wells having elevated arsenic for all three thresholds. Birimian volcanites (basalt, andesite, rhyolite) and Birimian orthogneiss are also positive indicators for arsenic being above 5 and 10 $\mu\text{g/L}$. The higher the arsenic concentration, the fewer variables were significant in the model, with volcano-sedimentary schist being the dominant variable, causing a 4-fold and 17-fold increase in the odds of arsenic being above 10 $\mu\text{g/L}$ respectively 50 $\mu\text{g/L}$ (Table 5). The probability maps in Fig. 5 highlight areas that are vulnerable to elevated groundwater arsenic, showing probabilities of arsenic exceeding the specified threshold values.

The highest probabilities (0.7) are calculated for the threshold of 5 $\mu\text{g/L}$, meaning that there is a 70% chance of finding arsenic concentrations above 5 $\mu\text{g/L}$ in a well in this region. The low AUC value (0.57, Fig. 6) denotes rather poor discriminating power of the model. This is not surprising for this low threshold and reflects the nature of the calibration data: water with arsenic >5 $\mu\text{g/L}$ is well-represented in all rock types used as predictor variables, with only a slight preference for lithologies of the Birimian formation (Fig. 4). The lack of a clear, distinguishing predictor variable means that the specificity and sensitivity of the model are low, as high arsenic values are frequently classified into low-risk areas and vice-versa. The AUC for the 10 $\mu\text{g/L}$ model of 0.63 is also not very high. This also indicates that high arsenic values are often found outside the regions classified as “high risk”, reflecting the heterogeneity of the calibration dataset and the inability to find a clear predictor for high arsenic. Even though arsenic concentrations >10 $\mu\text{g/L}$ are mainly found in volcanites and volcano-sedimentary schist, some occurrences are also found in granitic rocks (granite and tonalite) (Fig. 4), which were not determined to be significant predictors. These arsenic measurements therefore plot as high values in low-risk areas, which reduces the model's specificity. The best AUC is calculated for the threshold of 50 $\mu\text{g/L}$, where volcano-sedimentary schists are the clearest predictor of high arsenic concentrations and the few high values are correctly classified.

Even though mineral deposits are hypothesised to be excellent proxies for mineralised zones, they were not a significant predictor for arsenic in the logistic regression model. This is not surprising when we consider that mineralised zones exist where mineral exploration may not have taken place yet or that are too limited in extent to be economical for mineral extraction. Nevertheless, such areas are still potential arsenic sources and may yield elevated groundwater arsenic concentrations even though they are not documented in the mineral deposits dataset. Most of the high-arsenic samples in the calibration dataset are from areas >10 km from documented mineral deposits. We therefore see the incompleteness of the mineral deposit dataset we used as the reason for its poor performance in predicting As-affected areas, and not the unsuitability of mineralised zones as As-predictors as such.

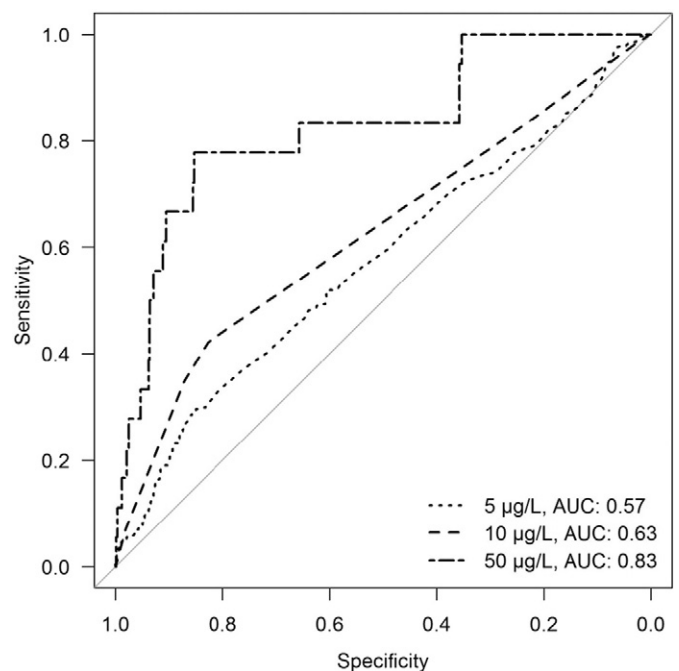


Fig. 6. Receiver operating characteristics (ROC) curves for the calculated logistic regression models using three different thresholds. The area under the curve (AUC) is displayed in the legend.

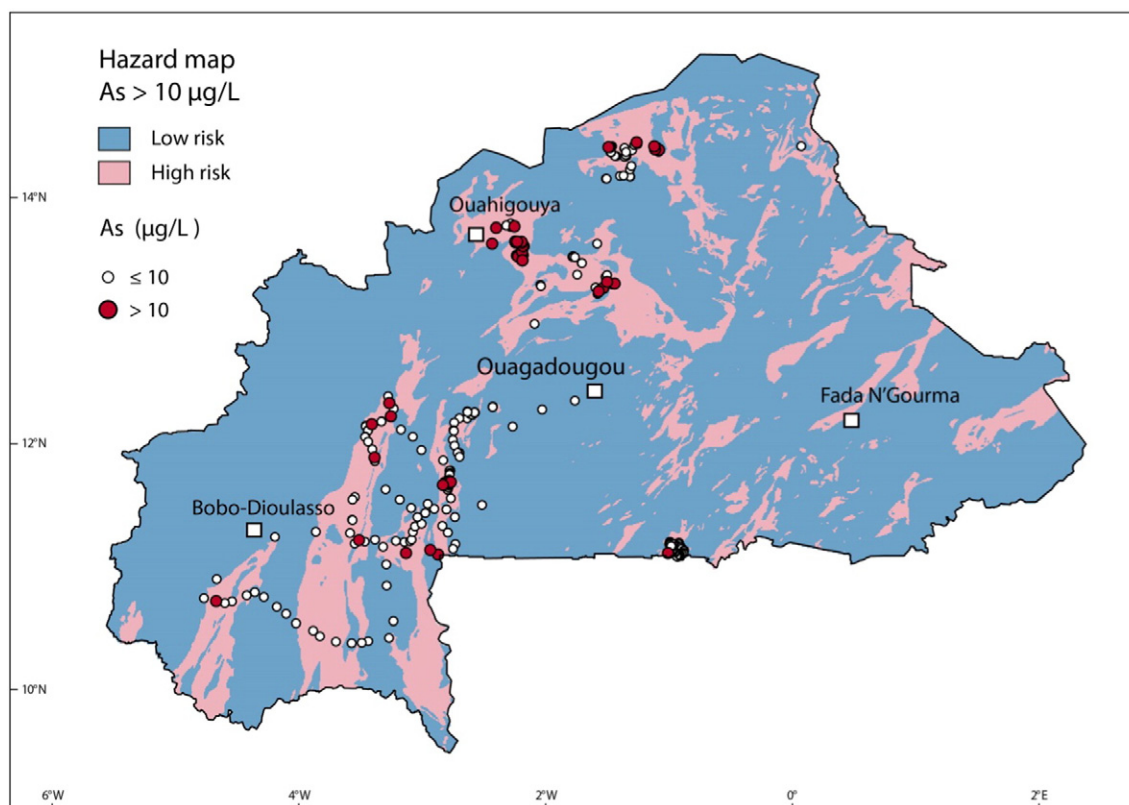


Fig. 7. Arsenic hazard map divided into “high” and “low” risk zones according to the probability cut-off of 0.2 of the 10 µg/L prediction model, overlain by the validation dataset of arsenic measurements ($n = 314$).

4.4. Model validation

The validation dataset, composed of 314 independent groundwater arsenic measurements was used to verify the validity of the prediction model in other regions of Burkina Faso outside of the geographical distribution of the calibration dataset. The validation data are located in the north, south and west of the country (Fig. 1) with 14% of concentrations above 10 µg/L. The 10 µg/L probability map was first classified into “high risk” and “low risk” zones by taking 0.2 as the probability cut-off value. The validation data were then plotted on this map and the rate of correct classification calculated (Fig. 7). Results presented in Table 6 show that 91% of high arsenic values (>10 µg/L) were correctly classified into high-risk areas (sensitivity, true positives), with only 9% plotting in low-risk regions (false negatives). For the low arsenic concentrations, 39% of these were correctly classified into low-risk areas (specificity, true negatives), with the remaining 61% in high risk areas (false positives). The high rate of false positives again reflects the nature of the arsenic concentration database, with only few high-arsenic wells being scattered among a majority of arsenic-safe wells. From a drinking water quality perspective, the high rate of false positives is less worrying, as finding good water quality in a high-risk area is a positive outcome. Much more important is the good performance of the model in predicting high-risk areas, with very few high-arsenic values plotting in low-risk areas.

Even though the presented hazard maps highlight areas at greater risk of arsenic contamination, they cannot accurately predict high arsenic concentrations of individual boreholes, since the spatial resolution of predictor variables is much coarser than the small-scale variability that can occur between boreholes. Such data cannot represent the extremely localised processes leading to highly varying arsenic concentrations in wells situated within hundreds of metres of each other. Ideally, to more accurately predict arsenic occurrence in Burkina Faso, one would need highly detailed maps of gold and/or sulphide mineral deposits (showing individual mineral veins) on a country-wide scale, as well as borehole logs showing the lithological structure and location of water-bearing fractures at depth.

4.5. Population at risk

Using large-scale and readily available geological data and a detailed dataset of arsenic measurements, we have produced a statistically sound hazard map predicting areas that are more likely to contain high concentrations of geogenic groundwater arsenic in Burkina Faso. By combining predicted high-risk areas (>20% chance of finding high arsenic concentrations) with population density, the total population at risk of drinking water elevated in arsenic (>10 µg/L) were estimated (Fig. 8). Burkina Faso sustains a largely rural population, with only 30% living in urban areas (UNICEF and World Health Organization,

Table 6
Model validation results.

Validation dataset, $n = 314$	No. of samples	Predicted > 10 µg/L (high risk)	Predicted ≤ 10 µg/L (low risk)
Observed > 10 µg/L (high As)	44	40 (91% true positives)	4 (9% false negatives)
Observed ≤ 10 µg/L (low As)	270	165 (61% false positives)	105 (39% true negatives)

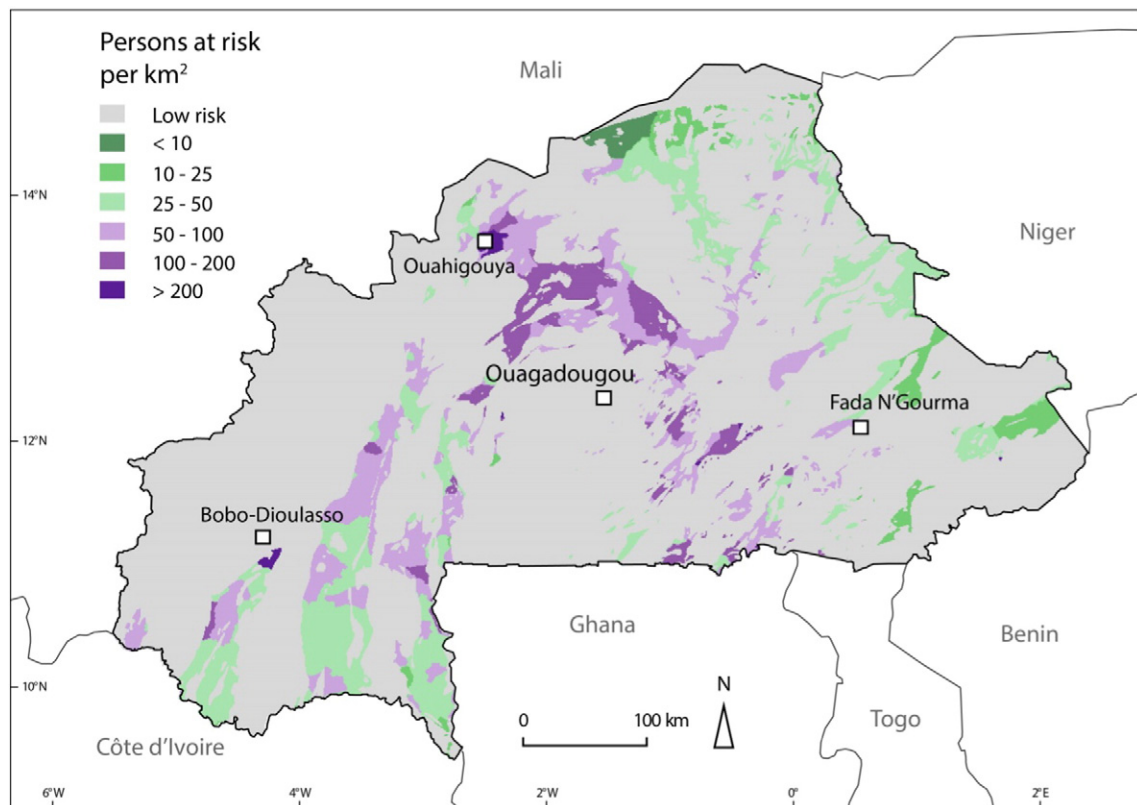


Fig. 8. Estimated number of persons at risk of being exposed to groundwater arsenic concentrations $>10 \mu\text{g/L}$ per km^2 in Burkina Faso. Population density data was retrieved from the Center for International Earth Science Information Network - CIESIN - Columbia University (2016).

2015). Altogether, about 4 million people, which is roughly one-fifth of the total population of 17.3 million, live in designated high-risk areas. Of these, 2.8 million are estimated to be rural inhabitants. Considering the calculated statistical probability that about 1 in 5 boreholes in these high-risk regions are contaminated with arsenic, about 560,000 people are potentially exposed to contaminated groundwater. Since groundwater is the main source of drinking water in rural areas and arsenic treatment techniques are as yet very rarely implemented, we consider this figure to be a valid estimate. This is a daunting number for one of the poorest and least-developed countries that is already facing numerous issues concerning water and sanitation (UNDP, 2015; UNICEF and World Health Organization, 2015). Even though large-scale targeted medical studies have not been undertaken to the authors' knowledge, arsenic-related health issues can be expected to be widespread and result in a considerable burden of disease and reduced productivity and life expectancy in the Burkinabè population. In addition, socio-economic, demographic and political conditions will contribute considerably to a population's total vulnerability to arsenic exposure (Singh and Vedwan, 2015).

4.6. Relevance for arsenic mitigation in Burkina Faso and the greater West African region

The presented arsenic hazard maps are aimed as a tool for water resource authorities to conduct drinking water surveys in areas where they are most needed. The testing of each drinking water well in high-risk regions is still necessary, as relatively few high-arsenic wells are generally distributed among many low-arsenic wells. The current practice is to close arsenic-affected wells with a chain or to dismantle them to prevent water abstraction by the population. Often a replacement well is not drilled in the vicinity, leading to water shortages and greatly increased walking distances

and hardship for women and children in charge of water collection. Closing a well without replacement only makes sense if an alternative, arsenic-free well is nearby, which may certainly be the case since several drinking water boreholes are often installed in a village.

Well-switching has proved to be a popular mitigation option in arsenic-affected regions in Bangladesh and is preferred over technological solutions such as water treatment filters (Ahmed et al., 2006; Inauen et al., 2013). Only where alternative, arsenic-safe wells are too far away does on-site arsenic treatment or the drilling of a new well make sense. Some success and encouraging results have already been seen in Burkina Faso with the installation of community-scale arsenic treatment filters by 2iE-Fondation based on commercially available iron-hydroxide filter materials, though this is not yet widespread (Ouedraogo, 2016). The installation of a filter needs careful operation and maintenance, trained local staff, frequent water quality monitoring, replacement of filter material when saturated, and, above all, the necessary funding for sustainable, long-term operation. These can be daunting tasks for remote rural communities and need to be addressed before any upscaling of filter techniques is possible. Therefore, switching to alternative, arsenic-free wells, where possible, is definitely the preferred mitigation option in Burkina Faso at the moment.

The arsenic hazard model generated may also be relevant in Burkina Faso's neighbouring countries, as the volcanites and volcano-sedimentary schists of the Birimian formation, which proved to be the most reliable predictor for high arsenic, also cover large areas of Ghana, the Ivory Coast, Mali, Niger and Benin. A transboundary hazard map for the whole West African region, calibrated and validated with local data would be a first step in creating awareness of geogenic arsenic contamination on a more regional scale and initiating necessary mitigation in affected areas.

Acknowledgements

The authors would like to thank Marcelle Ahissan, Lucien Stolze and Désiré Boro for assistance during field work in Burkina Faso. Thanks also goes to the NGOs “Le soleil dans la main” and “Fastenopfer” for taking water samples that complemented the arsenic concentration dataset, and to Pauline Smedley for permission to use arsenic data from her 2007 study. We acknowledge the laboratory staff at 2iE for storage of equipment and samples. Many thanks to Stephan Hug for useful comments that improved this manuscript and to Christian Zurbrugg for his helpful advice and diplomacy during the course of the project. Funding for this study was provided by the Swiss Agency for Development and Cooperation (SDC) through the Programme 3E (contract no. 81016359) and the Information Management System on Geogenic Contaminants, GAP (contract no. 81025383).

References

- Abraitis, P.K., Patrick, R.A.D., Vaughan, D.J., 2004. Variations in the compositional, textural and electrical properties of natural pyrite: a review. *Int. J. Miner. Process.* 74 (1–4), 41–59.
- Ahmed, K.M., Bhattacharya, P., Hasan, M.A., Akhter, S.H., Alam, S.M.M., Bhuyian, M.A.H., Imam, M.B., Khan, A.A., Sracek, O., 2004. Arsenic enrichment in groundwater of the alluvial aquifers in Bangladesh: an overview. *Appl. Geochem.* 19 (2), 181–200.
- Ahmed, M.F., Ahuja, S., Alauddin, M., Hug, S.J., Lloyd, J.R., Pfaff, A., Pichler, T., Saltikov, C., Stute, M., Van Geen, A., 2006. Ensuring safe drinking water in Bangladesh. *Science* 314 (5806):1687–1688. <http://dx.doi.org/10.1126/science.1133146>.
- Ahn, J.S., Cho, Y.C., 2013. Predicting natural arsenic contamination of bedrock groundwater for a local region in Korea and its application. *Environ. Earth Sci.* 68 (7), 2123–2132.
- Ahoulé, D., Lalanne, F., Mendret, J., Brosillon, S., Maïga, A., 2015. Arsenic in African waters: a review. *Water Air Soil Pollut.* 226 (9):1–13. <http://dx.doi.org/10.1007/s11270-015-2558-4>.
- Akaike, H., 1974. A new look at the statistical model identification. *IEEE Trans. Autom. Control* 19 (6):716–723. <http://dx.doi.org/10.1109/TAC.1974.1100705>.
- Alfredo, K.A., Lawler, D.F., Katz, L.E., 2014. Fluoride contamination in the Bongo District of Ghana, West Africa: geogenic contamination and cultural complexities. *Water Int.* 39 (4):486–503. <http://dx.doi.org/10.1080/02508060.2014.926234>.
- Amini, M., Abbaspour, K.C., Berg, M., Winkel, L., Hug, S.J., Hoehn, E., Yang, H., Johnson, C.A., 2008. Statistical modeling of global geogenic arsenic contamination in groundwater. *Environ. Sci. Technol.* 42 (10), 3669–3675.
- Apambire, W.B., Boyle, D.R., Michel, F.A., 1997. Geochemistry, genesis, and health implications of fluoriferous groundwaters in the upper regions of Ghana. *Environ. Geol.* 33 (1), 13–24.
- Argos, M., Kalra, T., Rathouz, P.J., Chen, Y., Pierce, B., Parvez, F., Islam, T., Ahmed, A., Rakibuz-Zaman, M., Hasan, R., Sarwar, G., Slavkovich, V., Van Geen, A., Graziano, J., Ahsan, H., 2010. Arsenic exposure from drinking water, and all-cause and chronic-disease mortalities in Bangladesh (HEALS): a prospective cohort study. *Lancet* 376 (9737), 252–258.
- Asante, K.A., Agusa, T., Subramanian, A., Ansa-Asare, O.D., Biney, C.A., Tanabe, S., 2007. Contamination status of arsenic and other trace elements in drinking water and residents from Tarkwa, a historic mining township in Ghana. *Chemosphere* 66 (8), 1513–1522.
- Ayotte, J.D., Nolan, B.T., Nuckols, J.R., Cantor, K.P., Robinson Jr., G.R., Baris, D., Hayes, L., Karagas, M., Bress, W., Silverman, D.T., Lubin, J.H., 2006. Modeling the probability of arsenic in groundwater in New England as a tool for exposure assessment. *Environ. Sci. Technol.* 40 (11), 3578–3585.
- Ayotte, J.D., Nolan, B.T., Gronberg, J.A., 2016. Predicting arsenic in drinking water wells of the Central Valley, California. *Environ. Sci. Technol.* 50 (14):7555–7563. <http://dx.doi.org/10.1021/acs.est.6b01914>.
- Barro-Traoré, F., Tiendrébéogo, S.R.M., Lallogo, S., Tiendrébéogo, S., Dabal, M., Ouedraogo, H., 2008. Manifestations cutanées de l'arcanisme au Burkina Faso: aspects épidémiologiques et cliniques. *Mali Medical, Tome. XXIII* (1).
- Berg, M., Stengel, C., Trang, P.T.K., Hung Viet, P., Sampson, M.L., Leng, M., Samreth, S., Fredericks, D., 2007. Magnitude of arsenic pollution in the Mekong and Red River Deltas - Cambodia and Vietnam. *Sci. Total Environ.* 372 (2–3), 413–425.
- Berg, M., Trang, P.T.K., Stengel, C., Buschmann, J., Viet, P.H., Van Dan, N., Giger, W., Stüben, D., 2008. Hydrological and sedimentary controls leading to arsenic contamination of groundwater in the Hanoi area, Vietnam: the impact of iron-arsenic ratios, peat, river bank deposits, and excessive groundwater abstraction. *Chem. Geol.* 249 (1–2): 91–112. <http://dx.doi.org/10.1016/j.chemgeo.2007.12.007>.
- Béziat, D., Dubois, M., Debat, P., Nikiéma, S., Salvi, S., Tollon, F., 2008. Gold metallogeny in the Birimian craton of Burkina Faso (West Africa). *J. Afr. Earth Sci.* 50 (2–4), 215–233.
- Bhattacharya, P., Chatterjee, D., Jacks, G., 1997. Occurrence of arsenic-contaminated groundwater in alluvial aquifers from delta plains, eastern India: options for safe drinking water supply. *Water Resour. Dev.* 13 (1):79–92. <http://dx.doi.org/10.1080/07900629749944>.
- Bourges, F., Debat, P., Tollon, F., Munoz, M., Ingles, J., 1998. The geology of the Taparko gold deposit, Birimian greenstone belt, Burkina Faso, West Africa. *Mineral. Deposita* 33 (6):591–605. <http://dx.doi.org/10.1007/s001260050175>.
- Buamah, R., Petrusovski, B., Schippers, J.C., 2008. Presence of arsenic, iron and manganese in groundwater within the gold-belt zone of Ghana. *J. Water Supply Res. Technol. AQUA* 57 (7), 519–529.
- Buschmann, J., Berg, M., Stengel, C., Sampson, M.L., 2007. Arsenic and manganese contamination of drinking water resources in Cambodia: coincidence of risk areas with low relief topography. *Environ. Sci. Technol.* 41 (7), 2146–2152.
- Castaigne, C., Billa, M., Milesi, J.P., Thieblemont, D., Le Metour, J., Egal, E., Donzeau, M., Buerrrot, C., Cocherie, A., Chevremont, P., Tegye, M., Itard, Y., Zida, B., Ouedraogo, I., Kote, S., Kabore, B.E., Ouedraogo, C., Ki, J.C., Zunino, C., 2003a. Notice explicative de la Carte géologique et minière du Burkina Faso à 1/1 000 000. Ouagadougou, Burkina Faso.
- Castaigne, C., Le Metour, J., Billa, M., Donzeau, M., Chevremont, P., Egal, E., Zida, B., Ouedraogo, I., Kote, S., Kabore, B.E., Ouedraogo, C., Thieblemont, D., Guerot, C., Cocherie, A., Tegye, M., Milesi, J.P., Itard, Y., 2003b. Carte géologique et minière du Burkina Faso à 1/1 000 000. Ouagadougou, Burkina Faso.
- Center for International Earth Science Information Network - CIESIN - Columbia University, 2016k. Gridded Population of the World, Version 4 (GPWv4): Population Density (Retrieved from: <http://dx.doi.org/10.7927/H4NP22DQ>).
- Courtois, N., Lachassagne, P., Wynn, R., Blanchin, R., Bougaïré, F.D., Somé, S., Tapsoba, A., 2010. Large-scale mapping of hard-rock aquifer properties applied to Burkina Faso. *Ground Water* 48 (2), 269–283.
- COWI, 2004. Etude sur l'arsenic dans l'eau souterraine de la zone du PEEN COWI Engineering, Programme Eau et Environnement - Région du Nord : Ministère de l'Agriculture, de l'Hydraulique et des Ressources Halieutiques - Burkina Faso. Copenhagen.
- Dewandel, B., Maréchal, J.C., Bour, O., Ladouche, B., Ahmed, S., Chandra, S., Pauwels, H., 2012. Upscaling and regionalizing hydraulic conductivity and effective porosity at watershed scale in deeply weathered crystalline aquifers. *J. Hydrol.* 416–417:83–97. <http://dx.doi.org/10.1016/j.jhydrol.2011.11.038>.
- Dixit, S., Hering, J.G., 2003. Comparison of arsenic(V) and arsenic(III) sorption onto iron oxide minerals: implications for arsenic mobility. *Environ. Sci. Technol.* 37 (18), 4182–4189.
- Dummer, T.J.B., Yu, Z.M., Nauta, L., Murimboh, J.D., Parker, L., 2015. Geostatistical modelling of arsenic in drinking water wells and related toenail arsenic concentrations across Nova Scotia, Canada. *Sci. Total Environ.* 505:1248–1258. <http://dx.doi.org/10.1016/j.scitotenv.2014.02.055>.
- Edmunds, W.M., 2008. In: Adelana, S., MacDonald, A. (Eds.), *Groundwater in Africa - palaeowater, climate change and modern recharge*. Applied Groundwater Studies in Africa: Taylor & Francis.
- Fawcett, T., 2006. An introduction to ROC analysis. *Pattern Recogn. Lett.* 27 (8):861–874. <http://dx.doi.org/10.1016/j.patrec.2005.10.010>.
- Fendorf, S., Michael, H.A., Van Geen, A., 2010. Spatial and temporal variations of groundwater arsenic in South and Southeast Asia. *Science* 328 (5982), 1123–1127.
- Filippi, C., Milville, F., Thiery, D., 1990. Evaluation of natural recharge to aquifers in the Sudan-Sahel climate using global hydrological modelling: application to ten sites in Burkina Faso. *Hydrol. Sci. J.* 35 (1):29–48. <http://dx.doi.org/10.1080/02626669009492403>.
- Flanagan, S.V., Johnston, R.B., Zheng, Y., 2012. Arsenic in tube well water in Bangladesh: health and economic impacts and implications for arsenic mitigation. *Bull. World Health Organ.* 90 (11):839–846. <http://dx.doi.org/10.2471/blt.11.101253>.
- GRASS Development Team, 2015. *Geographic Resources Analysis Support System (GRASS) Software, Version 7.0: Open Source Geospatial Foundation* (Retrieved from <http://grass.osgeo.org>).
- Hosmer, D.W., Lemeshow, S., Sturdivant, R.X., 2013. *Applied Logistic Regression*. vol. 398. John Wiley & Sons.
- Hu, Z., Gao, S., 2008. Upper crustal abundances of trace elements: a revision and update. *Chem. Geol.* 253 (3–4):205–221. <http://dx.doi.org/10.1016/j.chemgeo.2008.05.010>.
- Hug, S.J., Leupin, O., 2003. Iron-catalyzed oxidation of arsenic(III) by oxygen and by hydrogen peroxide: pH-dependent formation of oxidants in the Fenton reaction. *Environ. Sci. Technol.* 37 (12):2734–2742. <http://dx.doi.org/10.1021/es026208x>.
- Huneau, F., Dakoure, D., Celle-Jeanton, H., Vitvar, T., Ito, M., Traore, S., Compaore, N.F., Jirakova, H., Le Coustumer, P., 2011. Flow pattern and residence time of groundwater within the south-eastern Taoudeni sedimentary basin (Burkina Faso, Mali). *J. Hydrol.* 409 (1–2), 423–439.
- Inauen, J., Hossain, M.M., Johnston, R.B., Mosler, H.J., 2013. Acceptance and use of eight arsenic-safe drinking water options in Bangladesh. *PLoS One* 8 (1). <http://dx.doi.org/10.1371/journal.pone.0053640>.
- Lehner, B., Verdin, K., Jarvis, A., 2008. New global hydrography derived from spaceborne elevation data. *Eos* 89 (10), 93–94.
- MacDonald, A.M., Calow, R.C., 2009. Developing groundwater for secure rural water supplies in Africa. *Desalination* 248 (1–3):546–556. <http://dx.doi.org/10.1016/j.desal.2008.05.100>.
- MacDonald, A.M., Calow, R.C., MacDonald, D.M.J., Darling, W.G., Dochartaigh, B.E.O., 2009. What impact will climate change have on rural groundwater supplies in Africa? *Hydrol. Sci. J.* 54 (4):690–703. <http://dx.doi.org/10.1623/hysj.54.4.690> (Journal Des Sciences Hydrologiques).
- MAHRH/MS, 2005. Arrêté Conjoint n°0019/MAHRH/MS du 5 avril 2005 portant définition des normes de potabilité de l'eau. Ministère de l'Agriculture, de l'Hydraulique et de Ressources Halieutiques du Burkina Faso, Ministère de la Santé du Burkina Faso (Retrieved 01.11.2016, from http://www.legiburkina.bf/m/Sommaires_JO/Arr%C3%AAt%C3%A9_n_conjoint_MHRH_MS_2005_00019.htm).
- Martin, N., Van De Giesen, N., 2005. Spatial distribution of groundwater production and development potential in the Volta River basin of Ghana and Burkina Faso. *Water Int.* 30 (2), 239–249.

- Milési, J.P., Ledru, P., Feybesse, J.L., Dommanget, A., Marcoux, E., 1992. Early proterozoic ore deposits and tectonics of the Birimian orogenic belt, West Africa. *Precambrian Res.* 58 (1–4), 305–344.
- Naujokas, M.F., Anderson, B., Ahsan, H., Aposhian, H.V., Graziano, J.H., Thompson, C., Suk, W.A., 2013. The broad scope of health effects from chronic arsenic exposure: update on a worldwide public health problem. *Environ. Health Perspect.* 121 (3):295–302. <http://dx.doi.org/10.1289/ehp.1205875>.
- Nikiema, J., Schirmer, M., Gläßer, W., Krieg, R., 2010. Correlative and comparative characterization of main ion concentrations in laterite groundwater in semi-arid northern Burkina Faso. *Environ. Earth Sci.* 61 (1), 11–26.
- Nikiema, J., Gläßer, W., Krieg, R., Schirmer, M., 2013. Trace elements and their correlations in hand-dug wells in a laterite environment in a semi-arid region: case study of Tikaré, Northern Burkina Faso. *Environ. Earth Sci.* 69 (7), 2393–2414.
- Nolan, B.T., Hitt, K.J., 2006. Vulnerability of shallow groundwater and drinking-water wells to nitrate in the United States. *Environ. Sci. Technol.* 40 (24):7834–7840. <http://dx.doi.org/10.1021/es060911u>.
- Nolan, B.T., Hitt, K.J., Ruddy, B.C., 2002. Probability of nitrate contamination of recently recharged groundwaters in the conterminous United States. *Environ. Sci. Technol.* 36 (10):2138–2145. <http://dx.doi.org/10.1021/es0113854>.
- Nzihou, J.F., Bouda, M., Hamidou, S., Diarra, J., 2013. Arsenic in drinking water toxicological risk assessment in the north region of Burkina Faso. *J. Water Resour. Protect.* 5 (8A), 46.
- Ouedraogo, S.B.E., 2016. Étude du fonctionnement d'un procédé de traitement de l'arsenic par adsorption sur oxyde de fer. (Unpublished Master thesis), Institut International d'Ingénierie de l'Eau et de l'Environnement (2iE), Ouagadougou, Burkina Faso.
- Ouedraogo, O., Amyot, M., 2013. Mercury, arsenic and selenium concentrations in water and fish from sub-Saharan semi-arid freshwater reservoirs (Burkina Faso). *Sci. Total Environ.* 444, 243–254.
- Ouedraogo, I., Defourny, P., Vanclooster, M., 2016. Mapping the groundwater vulnerability for pollution at the pan African scale. *Sci. Total Environ.* 544:939–953. <http://dx.doi.org/10.1016/j.scitotenv.2015.11.135>.
- QGIS Development Team, 2015. QGIS Geographic Information System: Open Source Geospatial Foundation (Retrieved from <http://www.qgis.org/>).
- R Core Team, 2015. A Language and Environment for Statistical Computing. R Foundation for Statistical Computing, Vienna, Austria (Retrieved from <http://www.R-project.org/>).
- Rodríguez-Lado, L., Sun, G., Berg, M., Zhang, Q., Xue, H., Zheng, Q., Johnson, C.A., 2013. Groundwater arsenic contamination throughout China. *Science* 341 (6148), 866–868.
- Sako, A., Bamba, O., Gordio, A., 2016. Hydrogeochemical processes controlling groundwater quality around Bomboré gold mineralized zone, Central Burkina Faso. *J. Geochem. Explor.* 170:58–71. <http://dx.doi.org/10.1016/j.gexplo.2016.08.009>.
- Salifu, A., Petrushevski, B., Ghebremichael, K., Buamah, R., Amy, G., 2012. Multivariate statistical analysis for fluoride occurrence in groundwater in the Northern region of Ghana. *J. Contam. Hydrol.* 140–141, 34–44.
- Schlüter, T., 2008. *Geological Atlas of Africa*. Springer.
- Shamsudduha, M., Taylor, R.G., Chandler, R.E., 2015. A generalized regression model of arsenic variations in the shallow groundwater of Bangladesh. *Water Resour. Res.* <http://dx.doi.org/10.1002/2013WR014572>.
- Singh, S.K., Vedwan, N., 2015. Mapping composite vulnerability to groundwater arsenic contamination: an analytical framework and a case study in India. *Nat. Hazards* 75 (2):1883–1908. <http://dx.doi.org/10.1007/s11069-014-1402-2>.
- Smedley, P.L., 1996. Arsenic in rural groundwater in Ghana. *J. Afr. Earth Sci.* 22 (4), 459–470.
- Smedley, P.L., Knudsen, J., Maiga, D., 2007. Arsenic in groundwater from mineralised Proterozoic basement rocks of Burkina Faso. *Appl. Geochem.* 22 (5), 1074–1092.
- Smith, A.H., Lingas, E.O., Rahman, M., 2000. Contamination of drinking-water by arsenic in Bangladesh: a public health emergency. *Bull. World Health Organ.* 78 (9), 1093–1103.
- Somé, I., Sakira, A., Ouédraogo, M., Ouédraogo, T., Traoré, A., Sondo, B., Guissou, P., 2012. Arsenic levels in tube-wells water, food, residents' urine and the prevalence of skin lesions in Yatenga province, Burkina Faso. *Interdiscip. Toxicol.* 5 (1), 38–41.
- Sorichetta, A., Ballabio, C., Masetti, M., Robinson, G.R., Sterlacchini, S., 2013. A comparison of data-driven groundwater vulnerability assessment methods. *Groundwater* 51 (6): 866–879. <http://dx.doi.org/10.1111/gwat.12012>.
- UNDP, 2015. Human Development Report 2015. United Nations Development Programme, New York, USA.
- UNICEF, 2008. *UNICEF Handbook on Water Quality*. United Nations Children's Fund, New York/USA.
- UNICEF and World Health Organization, 2015. *Progress on Sanitation and Drinking Water: 2015 Update and MDG Assessment*. World Health Organization (WHO), Geneva.
- Van Geen, A., Zheng, Y., Versteeg, R., Stute, M., Horneman, A., Dhar, R., Steckler, M., Gelman, A., Small, C., Ahsan, H., Graziano, J.H., Hussain, I., Ahmed, K.M., 2003. Spatial variability of arsenic in 6000 tube wells in a 25 km² area of Bangladesh. *Water Resour. Res.* 39 (5), HWC31–HWC316.
- Verplanck, P.L., Mueller, S.H., Goldfarb, R.J., Nordstrom, D.K., Youcha, E.K., 2008. Geochemical controls of elevated arsenic concentrations in groundwater, Ester Dome, Fairbanks district, Alaska. *Chem. Geol.* 255 (1–2):160–172. <http://dx.doi.org/10.1016/j.chemgeo.2008.06.020>.
- Walker, F.P., Schreiber, M.E., Rimstidt, J.D., 2006. Kinetics of arsenopyrite oxidative dissolution by oxygen. *Geochim. Cosmochim. Acta* 70 (7):1668–1676. <http://dx.doi.org/10.1016/j.gca.2005.12.010>.
- WHO, 2011. *Guidelines for Drinking-Water Quality*. World Health Organization, Geneva, Switzerland.
- Winkel, L., Berg, M., Amini, M., Hug, S.J., Annette Johnson, C., 2008. Predicting groundwater arsenic contamination in Southeast Asia from surface parameters. *Nat. Geosci.* 1 (8), 536–542.
- Winkel, L.H.E., Trang, P.T.K., Lan, V.M., Stengel, C., Amini, M., Ha, N.T., Viet, P.H., Berg, M., 2011. Arsenic pollution of groundwater in Vietnam exacerbated by deep aquifer exploitation for more than a century. *Proc. Natl. Acad. Sci. U. S. A.* 108 (4), 1246–1251.
- Yang, Q., Jung, H.B., Marvinney, R.G., Culbertson, C.W., Zheng, Y., 2012. Can arsenic occurrence rates in bedrock aquifers be predicted? *Environ. Sci. Technol.* 46 (4), 2080–2087.
- Yang, Q., Culbertson, C.W., Nielsen, M.G., Schalk, C.W., Johnson, C.D., Marvinney, R.G., Stute, M., Zheng, Y., 2015. Flow and sorption controls of groundwater arsenic in individual boreholes from bedrock aquifers in central Maine, USA. *Sci. Total Environ.* 505: 1291–1307. <http://dx.doi.org/10.1016/j.scitotenv.2014.04.089>.
- Yuan, Y., Marshall, G., Ferreccio, C., Steinmaus, C., Selvin, S., Liaw, J., Bates, M.N., Smith, A.H., 2007. Acute myocardial infarction mortality in comparison with lung and bladder cancer mortality in arsenic-exposed region II of Chile from 1950 to 2000. *Am. J. Epidemiol.* 166 (12), 1381–1391.
- Yuan, Y., Marshall, G., Ferreccio, C., Steinmaus, C., Liaw, J., Bates, M., Smith, A.H., 2010. Kidney cancer mortality fifty-year latency patterns related to arsenic exposure. *Epidemiology* 21 (1):103–108. <http://dx.doi.org/10.1093/EDE.0b013e3181c21e46>.